

1 **Hydrogen evolution in microbial electrolysis cells treating landfill**  
2 **leachate: dynamics of anodic biofilm**

3  
4 Muhammad Hassan<sup>a,b</sup>, Ana Sotres Fernandez<sup>a</sup>, Isabel San Martin<sup>a</sup>, Bing Xie<sup>b</sup>, Antonio  
5 Moran\*<sup>a</sup>

6 <sup>a</sup>Chemical and Environmental Bioprocess Engineering Group, Natural Resources  
7 Institute (IRENA), Universidad de Leon, Avda. de Portugal 41, Leon 24009, Spain

8  
9 <sup>b</sup>Shanghai Key Laboratory for Urban Ecological Process and Eco-Restoration, School of  
10 Ecology & Environmental Sciences, East China Normal University Shanghai 200241, PR  
11 China

12  
13  
14  
15 \*Corresponding author, Email: [amorp@unileon.es](mailto:amorp@unileon.es), Phone: [+34 987 291841](tel:+34987291841)

16  
  
17 Intended for: **International Journal of Hydrogen Energy**

18 Type of contribution: **Research Article**

19 **Abstract**

20 Two microbial electrolysis cells (MEC-1 and 2) under 30 °C and 17±3 °C temperatures,  
21 respectively were operated using simulated landfill leachate as substrate. The system  
22 achieved a projected current density of 1000–1200 mA m<sup>-2</sup> (MEC-1) and 530–755 mA  
23 m<sup>-2</sup> (MEC-2) coupled with low cost hydrogen production rate of 0.148 L La<sup>-1</sup> d<sup>-1</sup> (MEC-  
24 1) and 0.04 L La<sup>-1</sup> d<sup>-1</sup> (MEC-2) at an applied voltage of 1.0 V. Current generation led to  
25 a maximum COD oxidation of 73±8% (MEC-1) and 65±7% (MEC-2) with ≥100%  
26 energy recovery. The system also exhibited a high hydrogen recovery (66–95%), pure  
27 hydrogen yield (98%) and tremendous working stability during two months of operation.  
28 Electroactive microbes such as *Pseudomonadaceae*, *Geobacteraceae* and  
29 *Comamonadaceae* were found in anodophilic biofilm, along with *Rhodospirillaceae* and  
30 *Rhodocyclaceae*, which could be involved in hydrogen production. These results  
31 demonstrated an energy-efficient approach for hydrogen production coupled with  
32 pollutants removal.

33

34 **Keywords:** Microbial electrolysis cells (MECs), energy efficiency, landfill leachate,  
35 Pyrosequencing, Hydrogen

36

37 **Nomenclature:**

38

---

BES	bioelectrochemical system
MEC	microbial electrolysis cell
DNA	deoxyribo nucleic acid
rRNA	ribosomal ribonucleic acid
PBS	phosphate buffered solution
PCR	polymerase chain reaction
$r_{cat}$	cathodic hydrogen recovery
OTUs	operational taxonomic units
Anammox	anaerobic ammonium oxidation
CEM	cationic exchange membrane
HRT	hydraulic retention time

---

39

40 **Glossary:**

- 41 • CE (Coulombic efficiency): the ratio of total coulombs actually transferred to the  
42 anode from the substrate to the maximum possible coulombs if all substrate  
43 removal produces electricity.
- 44 •  $E_{sp}$  (Specific energy consumption): the electrical energy consumed per kg of COD  
45 removed.
- 46 •  $\eta_E$  (Energy recovery efficiency): ratio of electrical energy output in terms of  $H_2$   
47 and  $CH_4$  gases to electrical energy input.
- 48 • MEC (Microbial electrolysis cell): bioelectrochemical system, which is used to  
49 produce hydrogen ( $H_2$ ) and other value - added chemicals.
- 50 •  $QH_2$  (Volumetric hydrogen evolution): the total amount of hydrogen produced per  
51 day and per liter of anodic chamber.

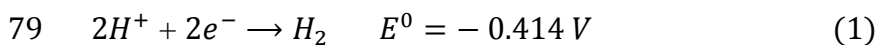
52

53 **Highlights**

- 54 • Simulated landfill leachate was employed as substrate for H<sub>2</sub> production in MEC.
- 55 • The system showed a high H<sub>2</sub> recovery (66-95%) and pure H<sub>2</sub> yield (98%).
- 56 • Applied potential, temperature and organic load imparted clear affect on system
- 57 efficiency.
- 58 • Low cost and pure H<sub>2</sub> yield was attained having less energy consumption.
- 59 • Anodophilic communities shared 33.7% of the total OTUs showing quite stable
- 60 over time

## 61 1. Introduction

62 Environmental pollution and energy shortages are two major global puzzles of the  
63 time. The present energy mainly comes from burning fossil fuels; however, depletion of  
64 fossil reserves with burgeoning global energy demand and increasingly environmental  
65 pollution is a matter of concern. Hence, the demand of renewable energy resources to  
66 replace fossil fuels has attracted worldwide attention. Hydrogen gas (H<sub>2</sub>) is a preferred  
67 alternate energy source since it is clean and renewable energy carrier. Nowadays, H<sub>2</sub> gas  
68 is mostly produced from certain processes such as gasification, pyrolysis,  
69 thermochemical water splitting, steam reformation, electrolysis, fermentation and photo-  
70 fermentation [1]. One very promising technology to generate bio hydrogen gas is the use  
71 of microbial electrolysis cell (MEC), a viable alternative for wastewater treatment as well  
72 [2–4]. The H<sub>2</sub> evolution rates are significantly higher in MECs (80 – 100%) as compared  
73 to the fermentation process and water electrolysis [5]. In an MEC, a group of  
74 electroactive bacteria utilize the potential energy stored in the organic compounds to  
75 metabolize and grow, donating electrons to the anode which then transport to the cathode  
76 with anaerobic environment, through electrolyte in a circuit and generate H<sub>2</sub> gas  
77 electrochemically (i.e. electrohydrogenesis) by certain endergonic reactions [3,6], as  
78 described in Eq. (1).



80 The voltage produced by the exoelectrogenic bacteria is not sufficient for H<sub>2</sub> gas  
81 evolution, therefore in most cases, MECs a certain external voltage is added to the circuit  
82 to drive the redox reactions because no oxygen (or oxidative agent) is available in the  
83 cathode chamber electrochemical H<sub>2</sub> production [7]. Theoretically, a very low potential  
84 input (−0.414 V) is required to drive the process (Eq. 1), but in practice it is substantially

85 increased (i.e. 0.5 – 1.0 V) due to over potentials of the system. The H<sub>2</sub> production  
86 increases with the amplitude of applied potential ( $E_{ap}$ , 0.7 – 1.0 V), which still is quite  
87 lesser than required for water electrolysis (1.8 – 2.0 V) [4,6,8].

88 The electrohydrogenesis proficiencies differ significantly with the nature of  
89 substrates employed. The MEC system with easily biodegradable organic compounds  
90 would have high hydrogen yield and energy output. Nevertheless, upon employing  
91 wastewater as substrate, the performance might be worse due to the high vulnerability of  
92 electrochemically active microbiota [9]. As shown in Table 1, beside simple substrates, a  
93 broad range of complex substrates have been tested so far in MECs for  
94 electrohydrogenesis such as human urine, glycerol, starch, winery, food processing,  
95 domestic and industrial wastewaters. However, less attention was given to use landfill  
96 leachate as anodic substrate in MECs. Landfill leachate is a high strength wastewater  
97 with excessive COD, NH<sub>4</sub>-N and volatile fatty acid contents (VFAs). Organic content  
98 present in landfill leachate and its composition vary depending on the type of landfill  
99 waste materials and age of the leachate. High COD (>5 g L<sup>-1</sup>) and NH<sub>4</sub>-N (> 0.4 g L<sup>-1</sup>)  
100 content, and low BOD<sub>5</sub>/COD ratio (< 0.1) makes biological treatment of landfill leachate  
101 very difficult [10,11].

102 <Table 1>

103 Employing landfill leachate as raw material for production of energy and  
104 chemicals is a novel approach. It is likely that landfill leachates with unique  
105 physiochemical characteristics and more complex components have higher difficulties in  
106 hydrogen production. Whether or not MEC system can catalyze landfill leachate to  
107 produce H<sub>2</sub> gas is still dubious owing to least attention. Anode respiring bacteria (ARB),  
108 the key microbes that colonize the anode of BES, can oxidize only a few simple  
109 compounds as electron donors. In this regard, Mahmoud et al. [12] employed pre-

110 fermentation of mature landfill leachate (BOD<sub>5</sub>/COD ratio of 0.32) for enhanced current  
111 density, CE and organics removal in MEC. The fermentation reactions produce the  
112 mixture of simpler compounds that ARB can oxidize. During fermentation, the complex  
113 organic compounds in the leachate were converted to simple VFAs, mainly succinate and  
114 acetate in batch tests, but mostly acetate in semi-continuous fermentation. The degree of  
115 conversion to VFAs improved by 4-fold, which led to a 68% increase in CE and a  
116 maximum current density of 23 A m<sup>-3</sup> (or 1.7 mA m<sup>-2</sup>). In another study [13], Fenton-  
117 based pre-treatment was employed to improve the biodegradability of landfill leachate  
118 that is subsequently fed to an MEC. It led to higher MEC performance: 52 ± 10% BOD<sub>5</sub>  
119 removal, 29 ± 3% CE, and 1.42 ± 0.27 A m<sup>-2</sup> current density as compared to 3 ± 0.3%  
120 BOD<sub>5</sub> removal, 1.8 ± 0.5% CE, and 0.11 ± 0.06 A m<sup>-2</sup> current density for the raw  
121 leachate.

122 Kargi et al. [14] employed landfill leachate for H<sub>2</sub> production applying DC  
123 voltage in the range of 0.5 – 5.0 V (i.e. electrohydrolysis) using aluminum electrodes.  
124 The highest cumulative H<sub>2</sub> evolution (5 L), H<sub>2</sub> yield (2.4 LH<sub>2</sub> g<sup>-1</sup> COD), daily H<sub>2</sub> gas  
125 production (1.27 Ld<sup>-1</sup>), and percent H<sub>2</sub> (99%) in the gas phase coupled with 77% COD  
126 removal were attained applying 4 V DC voltage. However, only 22 mL H<sub>2</sub> gas was  
127 generated within 96 h applying 0.5 V DC voltage. It indicated that the H<sub>2</sub> production was  
128 driven by electrohydrolysis other than bacterial decomposition of the leachate.

129 Since no MEC study has been employed for hydrogen production using landfill  
130 leachate as substrate. Herein, we investigate the potential opportunities of efficient clean  
131 hydrogen production treating simulated landfill leachate without any pre-treatment  
132 approach either biologically, physico-chemically or electro-chemically. To the best of our  
133 knowledge, this is the first study for H<sub>2</sub> evolution using landfill leachate as substrate.  
134 Series of batch scale experiments were conducted under different operational and

135 electrochemical conditions to see the overall system performance including organic and  
136 nitrogen content removal, energy consumption and yield. At the end, microbial  
137 community was studied for a better understanding of the H<sub>2</sub> generation mechanism.

## 138 **2. Materials and Methods**

### 139 **2.1 MEC set up**

140 A set of dual chambered rectangular reactors (MEC-1 and MEC-2) having 1.0 L  
141 and 0.5 L of total working volume, respectively as explained in previous work [15] was  
142 employed in this study. The schematics of experimental set-up is illustrated in Fig. 1. For  
143 hydrogen collection and measurement, the gas port at the top of cathode chamber was  
144 connected to an inverted measuring cylinder in a water tub. The anode of MEC-1 and  
145 MEC-2 consisted of 1.0 cm thick carbon felt (Sigratherm soft felt GFD 2, SGL Carbon  
146 Group, Wiesbaden, Germany), and the cathode was a perforated stainless steel plate with  
147 staggered-hole pattern, both with dimensions of 34.5 × 14.5 cm and 24.5 × 9.5 cm,  
148 respectively. The electrodes were separated by cation exchange membrane (CEM, CMI-  
149 7000, Membranes Int., USA). A titanium wire as current collector was connected with  
150 electrodes (two electrode system). The anolyte and catholyte in both systems was mixed  
151 with an external recirculation loop using a peristaltic pump (Dosiper C1R; Leon, Spain)  
152 at a recirculation rate of 8 L h<sup>-1</sup>, during batch and continuous mode of operation. Helium  
153 was purged into the anode and cathode stock solution bottles (5 L working volume) to  
154 ensure anaerobic conditions. A100 W heating pad (20×150 mm) (RoHS, UK) was fixed  
155 on the outer wall of anode chamber of MEC-1 to control the temperature at 30 °C.

156 <Fig. 1>

### 157 **2.2 MEC Operation**

158 The experiment was extended to a total duration of 62 days (MEC-1) and 58 days  
159 (MEC-2), operating under batch and continuous modes. Table 2 shows the various



160 conditions applied in MEC-1 and MEC-2. During the batch mode, the system was  
161 operated at a controlled temperature (30 °C, MEC-1) and room temperature (17±3 °C,  
162 MEC-2).

163 <Table 2>

164 During the inoculation period, the system was operated for 15 days (data not  
165 shown). Acetate (9.4 mM), propionate (1.8 mM) and glucose (1.5 mM) were used as  
166 carbon source with 1.0 mL<sup>-1</sup> of a trace metal solution, prepared according to Moreno et  
167 al. [16]. Nutrient buffer solution was (in g L<sup>-1</sup>) KH<sub>2</sub>PO<sub>4</sub>: 0.68, K<sub>2</sub>HPO<sub>4</sub>: 0.87, KCl: 0.74,  
168 NaCl: 0.58, MgSO<sub>4</sub>·7H<sub>2</sub>O: 0.1 and NH<sub>4</sub>Cl: 0.18, whereas 100 mM phosphate buffered  
169 solution (pH 7) was employed as catholyte. A 50 mL anaerobic digester sludge collected  
170 from municipal wastewater treatment plant of Leon (Spain) was used as inoculum in each  
171 reactor per liter of anode medium. A mean 75% of the media was replaced at the end of  
172 each batch cycle until a steady response of current production was observed.

173 After inoculation period, the simulated landfill leachate was employed as  
174 substrate prepared according to Rowe et al. [17] with minor modifications. The chemical  
175 characteristics of the simulated landfill leachate are presented in Table 3. In batch mode,  
176 100 mM PBS at pH 7 was used as catholyte and in continuous mode carbonate buffer  
177 (0.25 M NaHCO<sub>3</sub> and Na<sub>2</sub>CO<sub>3</sub>, pH 10) was applied.

178 <Table 3>

### 179 **2.3. Measurements and analytical determinations**

180 The MEC electrical outputs of each module were monitored separately. An  
181 adjustable DC power supply was used to maintain the voltage at a predetermined set  
182 point. The power supply was computer controlled using an analog output board (PCI-  
183 6713; National Instruments, Austin, TX). Data were recorded at 10 min intervals. The

184 produced gas in the cathode chambers was collected in 0.2 L gasbags and gas production  
185 rate was measured by inverted gas jar method.

186 Gas composition was analyzed by gas chromatography as described by Martinez  
187 et al. [18]. Ammonium nitrogen ( $\text{NH}_4\text{-N}$ ) was determined using an ion-selective electrode  
188 (781 pH/Ion Meter, Metrohm). The pH and conductivity were measured using pH meter  
189 and conductivity meter, respectively. Total organic carbon (TOC), total carbon (TC) and  
190 total nitrogen (TN) content were determined using a TOC analyzer (multi N/C 3100,  
191 AnalytikJena).

#### 192 **2.4. MEC performance parameters**

193 The MEC performance was evaluated in terms of (i) volumetric hydrogen yield  
194 ( $\text{QH}_2$ ) per liter of the reactor volume ( $\text{L a}^{-1} \text{ d}^{-1}$ ), (ii) coulombic efficiency (CE, %), the  
195 ratio between the total coulombs actually transferred to the anode from the substrate, and  
196 the theoretical maximum, (iii) cathodic  $\text{H}_2$  recovery ( $r_{\text{cat}}$ , %), calculated as the ratio of the  
197 electrons recovered as hydrogen gas to the total number of electrons that reach the  
198 cathode and (iv) specific energy consumption ( $E_{\text{sp}}$ ) expressed as the electrical energy  
199 consumed per kg of COD removed ( $\text{kW h kg-COD}^{-1}$ ), (v) net energy consumption ( $\text{kW h}$   
200  $\text{kg-COD}^{-1}$ ) and (vi) energy recovery efficiency ( $\eta_{\text{E}}$ , %). The computation methods for the  
201 aforementioned performance parameters have been explained in supplementary materials  
202 and derived from Ref. [4,19,20].

#### 203 **2.5. Microbial community analyses**

204 In order to study the microbial community attached to the electrodes at three  
205 different periods (PI, PII and PIII), three different spots of the anode carbon felt were  
206 sampled corresponding to 30, 42 and 62 days of operation. Samples PI and PII were  
207 taken during the continuous mode operation whereas, PIII corresponds to batch mode  
208 during the five months of total operation period. Further operating conditions are given in

209 Table S1 (supplementary material). Total genomic DNA was extracted with a PowerSoil®  
210 DNA Isolation Kit (MoBio Laboratories Inc., Carlsbad, CA, USA) following the  
211 manufacturer's instructions. The quantity and quality of the extracted DNA was checked  
212 measuring them in a NanoDrop 1000 (Thermo Scientific).

213 The DNA extracted was used for 454-pyrosequencing purposes. *16S rRNA* genes  
214 were amplified from each sample. The primer set used was 27Fmod (5-  
215 AGRGTTTGATCMTGGCTCAG-3`)/519R modBio (5-GTNTTACNGCGGCKGCTG-  
216 3`) for the eubacterial population. For amplification, 2µl of each DNA was used and a  
217 reaction was carried out in 50 µl containing 0.4 mM of fusion primers, 0.1 mM of  
218 dNTPs, 2.5 U of Taq ADN polymerase (Qiagen), and 5 µl of the reaction buffer  
219 (Qiagen). The PCR amplification was carried out in a thermocycler GeneAmp\_PCR  
220 system 9700 (Applied Biosystems) and operated with the following protocol: 30 s at 95  
221 °C, followed by 30 cycles at 94 °C for 30 s, annealing at 55 °C for 30 s, extension at 72  
222 °C for 10 min. The obtained DNA reads were compiled in FASTq files for further  
223 bioinformatic processing. These pyrosequencing data were also taxonomically classified  
224 using the Ribosomal Database Project Group (RDP), in order to compare the results  
225 obtained in both databases. The Venn diagram was performed using VENNY software,  
226 and XLSTAT software package was used for performing a Correspondence Analysis  
227 (CA). The data from pyrosequencing datasets was submitted to the Sequence Read  
228 Archive of the National Centre for Biotechnology Information (NCBI) for eubacterial  
229 populations.

## 230 **2.6 Statistical analysis**

231 Analysis of variance (ANOVA) with a significance level of 5% ( $p < 0.05$ ) was  
232 performed using Excel for Mac 2011 to determine statistical differences in the results  
233 obtained from different conditions.

## 234 **3 Results**

### 235 **3.1. Current generation**

236 Current response under each condition was monitored over time to evaluate the  
237 overall performance of the MEC configuration. Fig. 2A, B illustrates the variations of  
238 current intensity at various cycles in MEC-1 and MEC-2. Applied voltage ( $E_{ap}$ )  
239 statistically influenced the current density in both systems ( $p < 0.05$ ). As can be seen, the  
240 current density in MEC-1 rose to the highest value of 1000 – 1200 mA m<sup>-2</sup> in cycle 1 and  
241 2 (day 1–7), followed by 800 mA m<sup>-2</sup> in cycle 3 (day 7–16). Upon reducing the  $E_{ap}$  to 0.8  
242 V (cycle 4, day 17–22), a maximum current density of only 250 mA m<sup>-2</sup> was noticed  
243 followed by a two-fold surge in cycle 5. When the system was again run at  $E_{ap}$  of 1.0 V  
244 (cycle 6 and 7, day 32 – 47), the current density exhibited to a highest value of 800 mA  
245 m<sup>-2</sup>.

246 Similar trend was observed in MEC-2: the maximum current density attained was  
247 530 and 755 mA m<sup>-2</sup> (cycle 1–2, day 1–12) at 1.0 V  $E_{ap}$ , while only 485 – 510 mA m<sup>-2</sup>  
248 was registered at 0.8 V (cycle 3–4, day 13–24). The current intensity again increased to  
249 600 – 650 mA m<sup>-2</sup> at 1 V (cycle 5–6, day 25–40).

250 <Fig. 2>

### 251 **3.2. Organic and nitrogenous content removal**

252 Fig. 3A/B explains the COD removal rate at various operating cycles. The COD  
253 removal in MEC-1 (cycle 1–3) was in the range of 42 - 50% (1.12 – 1.17 g COD L<sup>-1</sup> d<sup>-1</sup>)  
254 (Fig. 3A). At 0.8 V, the COD removal efficacy substantially decreased to 15.1 – 32%  
255 (cycle 4–5) from an initial concentration of 6.74 – 11.11 g L<sup>-1</sup> d<sup>-1</sup>. The COD elimination  
256 further increased to 47±11 – 73±8% equating to 2.68±1.26 g COD L<sup>-1</sup> d<sup>-1</sup> (cycle 6–7) at  
257 1.0 V, describing that  $E_{ap}$  has statistical effect on COD removal ( $p < 0.01$ ). MEC-2  
258 demonstrated the same outcome ( $p < 0.01$ ), where 28.5 – 53.3% (cycle 1–2) was abated

259 from the similar initial concentrations as that of MEC-1 (Fig. 3B). In cycle 3 and 4 (0.8 V  
260 *E<sub>ap</sub>*) only a mean 13–15% COD removal was noticed which increased to 62±6% and  
261 65±7% COD abatement at a degradation rate of 1.53 g L<sup>-1</sup> d<sup>-1</sup> at *E<sub>ap</sub>* of 1.0 V.

262 It is found that the consumption order of complex ingredients in simulated  
263 leachate was acetic acid > butyric acid > propionic acid (data not shown), which is in  
264 accordance with Escapa et al. [15], where acetic and butyric acids were easily consumed  
265 and propionic acid exhibited a refractory behavior.

266 As expected, nitrogen revealed quite similar abatement trend as that of COD  
267 removal. At 1.0 V applied voltage, MEC-1 decreased the NH<sub>4</sub><sup>+</sup>-N concentration in the  
268 analyte from 788±163 to 232±120 mg L<sup>-1</sup>, representing a removal rate of 196±27 mg L<sup>-1</sup>  
269 d<sup>-1</sup> (72±5% efficiency) coupled with 36±11% NO<sub>3</sub><sup>-</sup>-N reduction (12±2 mgL<sup>-1</sup> d<sup>-1</sup>)  
270 corresponding to a TN removal scale of 265±98 mg L<sup>-1</sup> d<sup>-1</sup> (Fig. 3C). The nitrogen at 0.8  
271 V exhibited slightly lower removal trend in both systems with a TN removal rate of  
272 62±12% and 48.5±0.8% in MEC-1 and 2, respectively. On the other hand, MEC-2  
273 presented 31 – 76% NH<sub>4</sub><sup>+</sup>-N removal (106±33 mgL<sup>-1</sup> d<sup>-1</sup>) followed by 29.3±18.3% NO<sub>3</sub><sup>-</sup>-  
274 N reduction (9.5±5.3 mgL<sup>-1</sup> d<sup>-1</sup>) constituting a TN degradation of 56.5±5.3% at a rate of  
275 146±83 mg L<sup>-1</sup> d<sup>-1</sup> (Fig. 3D).

276 <Fig 3>

### 277 3.3. Hydrogen production

278 In both MECs, hydrogen production in the cathode chamber followed the same  
279 trend as organic compounds removal regarding applied external voltages (*p* < 0.05). As  
280 shown in Table 4, higher hydrogen recoveries (*r<sub>cat</sub>*) in the range of 66 – 95% occurred  
281 with H<sub>2</sub> evolution of 0.08 – 0.148 L<sup>-1</sup> La<sup>-1</sup> d<sup>-1</sup> (at 1.0 V, MEC-1). However, at 0.8 V, *r<sub>cat</sub>*  
282 reduced to only 44 – 51% producing a mean QH<sub>2</sub> of 0.024 - 0.043 L La<sup>-1</sup> d<sup>-1</sup>. MEC-2  
283 exhibited low *r<sub>cat</sub>* of only 21 – 25% (cycle 1 and 2), followed by a surge to 120 and

284 114%, respectively with high rate of H<sub>2</sub> production in the last two subsequent cycles.  
285 When gas evolution started to enhance, pH and electrical conductivity (EC) in both  
286 systems rose up to 8.8 and 28 mS cm<sup>-1</sup> (MEC-1) and 10.19 and 26 mS cm<sup>-1</sup> (MEC-2)  
287 (results not shown).

288 <Table 4>

### 289 3.4. Energy balance and coulombic efficiency

290 Applied voltage exhibited a clear influence over energy balance as shown in Fig.  
291 4 At 1.0 V ≥ 100% energy recovery was achieved based on energy demand of 8.1×10<sup>-4</sup> to  
292 0.698 kWh-kg COD<sup>-1</sup> (MEC-1); whereas >100% energy efficiency was observed at 0.8 V  
293 having energy demand of 0.323 and 0.374 kWh-kg COD<sup>-1</sup> (MEC-1). The highest energy  
294 demand at cycle 3 might be due to very long cycle time of 230 h i.e. high-accumulated  
295 charge. In MEC-2, < 100% energy efficiency was observed at 1.0 and 0.8 V except cycle  
296 5 and 6, where highest efficiency of 139% was noticed with least energy consumption.  
297 The overall energy demand in MEC-1 was observed higher than MEC-2 having a similar  
298 trend in hydrogen production rate (Fig. 4).

299 <Fig 4>

300 Despite higher current densities, MEC-1 experienced low CEs (calculated with  
301 ΔCOD) in the range of 12 – 14.5% except cycle 3 (41%) at 1.0 V, and 18 – 20% at 0.8 V.  
302 On the other hand, MEC-2 exhibited 31% CE at the initial two cycles and increased to  
303 32.7 – 35.6% at *E<sub>ap</sub>* of 0.8V, but declined later (11 – 12.5%) at the terminal cycles (*E<sub>ap</sub>*  
304 = 1.0V) (Table 4).

### 305 3.5. Dynamics of anodic biofilm

306 Three anode samples were taken from the MEC-1 reactor at three different  
307 periods (PI, PII and PIII) along with inoculum sample in order to study the microbial

308 community composition attached onto the electrodes, and the similarities and differences  
309 between the eubacterial populations.

310 Firstly, to have an overall overview of the dynamics of the inoculum and the  
311 anode samples of MEC-1, correspondence analyses (CA) based on pyrosequencing  
312 results were carried out (Fig. 5A). The CA based on the relative abundances of the all  
313 genus presented in all samples. The sum of components (F1 and F2), explains 95% of the  
314 total variation among the samples. Over 100 genera were identified in all samples and  
315 used to do the matrix for the analysis, but just the main genera were represented in Fig.  
316 5A. Three clusters were obtained during these analyses. The inoculum cluster clearly  
317 differentiated from the other two, and the cluster composed for the MEC-1\_PI and MEC-  
318 1\_PII samples, which evolved towards a third cluster formed by MEC-1\_PIII sample.

319 To gain insights about the community structure of all samples that makes the  
320 differences between them, the phylogenetic composition at family level was analyzed and  
321 represented in Fig. 5B. The native microbiota of the initial inoculum from anaerobic  
322 digester showed differences respect to the anodophilic communities (MEC-1\_PI, MEC-  
323 1\_PII and MEC-1\_PIII). However, the three anodophilic samples taken showed quite  
324 similarities. Moreover, the family diversity is quite high such in the inoculum  
325 (represented by 17 families), as in the anode samples (18-21 different families) (Fig. 5B).

326 In the initial inoculum, 57% of the total community was accounted for four  
327 families i.e. *Eubacteriaceae* (22.2%), *Clostridiaceae* (14.5%), *Rhodocyclaceae* (11.0%)  
328 and *Comamonadaceae* (9.0%). In terms of composition, the three anodiphilic  
329 communities were similar between them, although the relative abundance of these  
330 families changed depending on the operational conditions. The dominant phyla identified  
331 in the anodic biofilm was *Proteobacteria*, represented by 11 families, some of them  
332 previously described in BES, such as *Pseudomonadaceae*, *Geobacteraceae*,

333 *Comamonadaceae*, *Rhodospirillaceae* and *Rhodocyclaceae* among others. *Bacteroidetes*  
334 and *Clostridia* were the other two dominant phyla identified.

335 <Fig 5>

336 In order to find out which OTUs showed a greater trend to establish themselves in  
337 anode biofilms, the presence of the common OTUs in the three different samples were  
338 compared among them (Fig. S1, supplementary material). The total amount of the  
339 observed OTUs in the three anodophilic biofilms were 1,572. The most part of these  
340 OTUs (604) were shared between MEC-1\_PI and MEC-1\_PII, representing to 38.4% of  
341 the total OTUs. Besides, a total of 529 OTUs, equivalent to 33.7% of the total community  
342 were shared between the three samples (MEC-1\_PI, MEC-1\_PII and MEC-1\_PIII). These  
343 OTUs, which prevailed attached onto the anode electrodes despite the different  
344 operational conditions, could be considered the core microbiome.

#### 345 **4. Discussions**

346 As it is clear from Fig. 2–4 and Table 4, the applied external voltage, temperature  
347 and influent COD content exhibited a clear impact on the overall system performance i.e.  
348 current density, substrate removal, energy consumption and hydrogen production. MEC  
349 current was generated by microbial oxidation of organic matter at the anode, and the  
350 presence of some microorganisms previously identified in BES as *Pseudomonadaceae*,  
351 *Comamonadaceae* and *Geobacteraceae*. The COD and nitrogen removal in the anode  
352 chamber increased with increasing current density [21], but prolong cycle durations as in  
353 cycle 3 (MEC-1) not only slow down the substrate removal rate but also the hydrogen  
354 production [22]. The system eliminated a maximum 77.5 and 65.7% COD, equating to  
355 treatment rate of 2.68 g COD L<sup>-1</sup> d<sup>-1</sup> and 1.53 g COD L<sup>-1</sup> d<sup>-1</sup> in MEC-1 and 2,  
356 respectively at  $E_{ap}$  of 1.0 V. As can be seen in Figure 3A/B, influent organic load has  
357 influenced the COD removal efficiency, suggesting that it may reach the saturation



358 conditions. Gil-Carrera et al. [23] found similar result in a semi-pilot scale MEC applying  
359 various organic loading rates.

360 On the basis of existing literature and operating conditions it is hypothesized that  
361 certain pathways might be involved in nitrogen removal in this study. As can be seen in  
362 Fig. 3C/D, the anolyte nitrogen removal was mainly attributed by  $\text{NH}_4^+\text{-N}$  in both  
363 systems. Ammonium transport to the cathode rises with increasing current density and it  
364 also depends on concentration gradient between anolyte and catholyte [21,24]. Although  
365 cathodic nitrogen content was not monitored in this study, however, the conductivity  
366 profiles in the anode and cathode chambers support this hypothesis. It was found that the  
367 conductivity of anolyte decreased from  $14.6\pm 2.3$  to  $10.3\pm 1.2$   $\text{mS cm}^{-1}$ , whereas catholyte  
368 conductivity increased from  $21.3\pm 1.1$  to  $28.6\pm 7.0$   $\text{mS cm}^{-1}$ . Nevertheless, this  
369 phenomenon was not merely attributed by  $\text{NH}_4^+\text{-N}$  migration but also ensured by other  
370 cations such as  $\text{Na}^+$ ,  $\text{K}^+$  and protons [25]. A little fraction of partial nitrification cannot be  
371 ruled out in the system as the reactor was exposed to oxygen prior to replenishment of the  
372 electrolyte in each batch cycle. In MECs, limited ammonium removal was observed with  
373 micro-aerobic conditions increasing the nitrification rate [26,27].  $\text{NH}_4^+\text{-N}$  removal can  
374 also be accomplished through bioelectrochemical denitrification and anammox process,  
375 since the anoxic/anaerobic anode chamber is best suited for such processes [28]. In an  
376 ammonium-fed MEC system, Zhan et al. [27] also observed ammonium oxidation in the  
377 presence of nitrite or nitrate under an applied voltage. Nitrate removal might be due to  
378 denitrification in the anode chamber as the presence of pseudomonads corroborates the  
379 process. The possible pathways of nitrogen removal from anodic chamber in MFC has  
380 been explained in our previous work [24], where young and old landfill leachate was  
381 employed as substrate.

382           Although MEC-2 consumed lower energy than MEC-1 but based on other  
383 efficiencies, like COD removal and hydrogen production, the later has been taken as a  
384 reference system during comparative evaluation with other systems/technologies. The  
385 reason why MEC-1 performed better than MEC-2 is because the former was controlled at  
386 30 °C whereas, the later at a wide range of room temperature (17±3 °C). Literature  
387 suggest that in BES, electrochemically active microbes rely upon an operational  
388 temperature of 30 °C [29,30]. At mesophilic conditions a clear specialization in  
389 anodophilic microorganisms were observed from cluster formed for inoculum sample to  
390 cluster formed for MEC-1\_PI and PII and the third group formed for MEC-1\_PIII (Fig.  
391 5A). Although the microbial diversity results similar both in the inoculum and in the  
392 biofilms samples, a clear enrichment in *Proteobacteria* phylum was observed. Some of  
393 well-known electroactive bacteria belong to this group as *Pseudomonadaceae*,  
394 *Comamonadaceae* and *Geobacteraceae* (Fig. 5B). The reason for such substantial decline  
395 in performance of MEC-2 could be the slower growth of electroactive bacteria. At cycle  
396 5 and 6 of MEC-2 there was an increase of the ambient temperature that can explain the  
397 improvement in the overall system efficiency. In this way not only applied voltage but  
398 also temperature exercised a clear impact on the system performance.

399           Coulombic efficiency (CE, %) is a parameter for the assessment of efficiently  
400 converting chemical energy stored in the substrate/wastewater into electrical energy, or in  
401 other words how much of the removed COD was converted to electrons. However in  
402 MECs, COD abatement is the main goal of wastewater treatment coupled with  
403 minimizing the overall energy demand for the process [22,31]. Low electrical energy  
404 input is more beneficial than high consumption of chemical energy (i.e. high CE) [30].  
405 The reason of low CEs at  $E_{ap}$  of 1.0 V despite higher current densities may reveal that a  
406 fraction of COD removed was due to certain other non-electrogenic activity. Another

407 possible reason might be the aerobic degradation of substrate sustained by oxygen  
408 intrusion, as the system was exposed to oxygen for 15 – 20 min prior to substrate  
409 replenishment in order to suppress methanogens [32]. In general, the long cycle time  
410 resulted in higher CEs, for example 41% in cycle 3 with total duration of 230 h. This  
411 phenomenon was in accordance with Wagner et al. [33] where highest CE was achieved  
412 in the long batch test of 184 h, having low recovery of hydrogen at the cathode (29±2%).

413         The high hydrogen recoveries in the MEC system was not only from high current  
414 densities but also owing to high conversion rate of electrons to hydrogen (i.e. cathodic  
415 hydrogen recoveries,  $r_{cat}$ ), meaning that 66 – 95% of the electrons captured from the  
416 substrate were transferred into current at  $E_{ap}$  of 1.0 V (Table 4). The gas production rate  
417 in both systems was highly variable based on applied voltage and cycle duration, for  
418 example at cycle 3 of MEC-1, long cycle time (230 h) resulted in a comparatively low  
419 recovery of hydrogen (76%), similar trend as observed by Wagner et al. [33]. However,  
420 the gas composition was consistent and highly enriched in H<sub>2</sub> (97 – 99%) along with 0.5–  
421 1.5% CH<sub>4</sub> and 0.5 – 1.0% CO<sub>2</sub>, revealing that the MEC system produced pure hydrogen  
422 gas. The intermittent oxygen exposure between batches may suppress methanogenic  
423 growth [19,34], hence very negligible portion of CH<sub>4</sub> appeared in the cathode. Moreover,  
424 operating MEC at a relative higher  $E_{ap}$  (> 0.6 V) is able to reduce methane production  
425 and improve the H<sub>2</sub> recovery [35], but higher than 1.0 V  $E_{ap}$  exhibit decrease in H<sub>2</sub> and  
426 increase in methane production [36]. The higher  $r_{cat}$  might also be linked to the  
427 phenomenon that no hydrogen recycling effect occurred between anode and cathode, as it  
428 is exhibited by lower CEs (< 100%).

### 429 **4.3. Comparative evaluation with other studies**

430         Table 5 shows the comparative evaluation of this study with other existing  
431 hydrogen producing technologies. Our results exhibited least energy requirements of 2.7

432 – 10.1 kWh-kg H<sub>2</sub> and higher energy recovery (MEC-1, 1.0 V *Eap*) than other  
433 technologies i.e. partial oxidation of heavy oils, coal gasification, steam methane  
434 reforming and grid water electrolysis. Moreover, the specific energy was below the net  
435 energy consumption threshold traditionally associated with aerobic treatment of domestic  
436 wastewater (0.7 - 2.0 kWh kg<sup>-1</sup> COD) [37]. The data of energy recovery suggested that  
437 MEC is an energy-producing device at 1.0 V *Eap*.

438         The estimated cost of hydrogen production via electrohydrogenesis due to the  
439 electrical energy input was lower than reported in literature. For example, using B-  
440 glycerol substrate, the energy cost was 0.945 € kg<sup>-1</sup> H<sub>2</sub> at applied voltage of 0.5 V and €  
441 1.11 kg<sup>-1</sup> H<sub>2</sub> at 0.9 V *Eap*, having energy demands of 2.32 kWh/m<sup>3</sup> H<sub>2</sub> (0.5 V *Eap*) and  
442 2.60 kWh/m<sup>3</sup> H<sub>2</sub> (0.9 V *Eap*), respectively [38]. These calculations were based on current  
443 wholesale electricity prices of € 38.65 per MWh, tax not included. Similarly, Battle-  
444 Vilanova et al. [39] estimated hydrogen production cost of 3.02 € kg<sup>-1</sup> H<sub>2</sub> at poised  
445 cathode potential of –1.0 V vs Ag/AgCl, and Cusick et al. [40] obtained comparatively  
446 low cost of 2.84 € kg<sup>-1</sup> H<sub>2</sub> for a MEC decontaminating domestic wastewater using a Pt  
447 catalyst. In this study, the energy cost was estimated to be 0.67±0.24 € kg<sup>-1</sup> H<sub>2</sub>  
448 (electricity prices of 150 € per MWh, tax included; www.omie.es) at energy demand of  
449 0.376±0.179 kWh per m<sup>3</sup> H<sub>2</sub>, which was even lower than H<sub>2</sub> production via steam  
450 methane reforming (0.71€ kg<sup>-1</sup> H<sub>2</sub>). In this way our system is accredited to produce low  
451 cost and pure hydrogen (≈99%) with low energy consumption.

452         Although MEC proved to be energy efficient technology but certain other  
453 parameters also need to be taken into consideration for practical applications of MECs  
454 like operating and capital costs, sludge production, environmental factors, HRTs and  
455 organics strength etc. Further research is required treating real wastewaters under realistic  
456 conditions in order to make this technique more viable. Moreover, correlating this

457 technology with certain other hydrogen producing technologies may give an  
458 understanding towards economical balanced hydrogen.

459

#### 460 **4.4. Challenges and future perspectives**

461 MEC technology is still in its infancy due to several inherent factors. The gap  
462 between rhetoric and reality in MEC research is substantial. This technology is mostly  
463 limited to the bench-scale studies ranging from a few milliliters to several liters at most.  
464 Although few researchers applied this technology in pilot-scale dealing with real  
465 wastewaters but were unable to attain a rational throughput. One more challenge which  
466 MECs confront is the start-up time ranging from weeks to months, which limits its  
467 practical application. Electrode materials and cathode catalysts are another concern in  
468 scaling-up this technology. Certain noble elements like platinum etc. have proved to be  
469 effective, however their high cost and short life time make them unreasonable for  
470 industrial-scale application. So far carbon-based materials are the most frequently  
471 employed electrodes due to their low cost and good biocompatibility, however high  
472 overpotentials and large ohmic/voltage loss make them less viable.

473 In this way, certain parameters need to be taken into consideration for practical  
474 applications of MECs like operating and capital costs, sludge production, environmental  
475 factors, HRTs and organics strength etc. Moreover, it needs further research treating real  
476 wastes under realistic conditions using plausible materials in order to make this  
477 technology reliable. As for as energy output in terms of hydrogen generation is  
478 concerned, correlating this technology with other existing techniques may give an  
479 understanding towards economical balance of the hydrogen.

480 Additive manufacturing or three-dimensional (3D) technology can be applied for  
481 electrode configuration, ion exchange membrane manufacturing or reactor designing. In  
482 MFCs, flat 2D porous anodes have small pore sizes, and bacteria can only clog on the  
483 surface and are out-of-the-way to the interior of the anode. This subsequently limits the  
484 anode efficacy. To overcome this glitch, 3D structured anodes have been devised, which  
485 provide larger bio-accessible area which promotes formation of active biofilm and  
486 effective substrate transfer simultaneously [41]. Moreover, Modeling and simulations  
487 may help design and refine such studies.

## 488 **5. Conclusion**

489 The system eliminated a maximum  $73\pm 8$  % COD, equating to treatment rate of  
490  $2.68 \text{ g COD L}^{-1} \text{ d}^{-1}$  (MEC-1) and  $65\pm 9\%$  (MEC-2) with least energy consumption. The  
491 overall energy demand in MEC-1 was observed higher than MEC-2. Applied voltage,  
492 temperature and HRT imparted a clear impact on the overall system efficiency. At  $1.0 \text{ V}$   
493  $E_{ap}$ , a maximum  $0.148 \text{ L H}_2 \text{ La}^{-1} \text{ d}^{-1}$  (MEC-1) and  $0.04 \text{ L H}_2 \text{ La}^{-1} \text{ d}^{-1}$  (MEC-2) was  
494 produced in batch mode. Nitrogen removal (mostly  $\text{NH}_4^+\text{-N}$ ) was occurred in the system  
495 obeying different removal pathways. The system also exhibited a high hydrogen recovery  
496 (66 – 95%), pure hydrogen yield (98%) and tremendous working stability during two  
497 months of operation. Regarding the eubacterial community, the native microbiota of the  
498 initial inoculum showed differences respect to the anodophilic communities which  
499 remain quite stable along different operational conditions, sharing 33.7% of the total  
500 OTUs. Besides, both electroactive and hydrogen producing bacteria were enriched at the  
501 anodic biofilm. The results of this study specified that MEC is an energy-efficient  
502 technique to deal with certain waste streams; however further research is needed treating  
503 real leachate under realistic conditions to make this technology reliable.  
504

505 **Acknowledgement**

506 This research was supported by the regional government ‘Junta de Castilla y Leon’ and  
507 Ana Sotres thanks for the postdoctoral contract associated with project reference:  
508 LE060U16 co-financed by FEDER funds. M.I. San Martin thanks the Spanish Ministry  
509 of Economy and Competitiveness the FPU fellowship granted (FPU13/04014).  
510 Muhammad Hassan wishes to thank East China Normal University, Shanghai-China for  
511 financial support through university’s study overseas program fund (40600-511232-  
512 14203/003) and National Science Foundation of China (31370510).

**References**

- 514 [1] Mahishi M. Theoretical and experimental investigation of hydrogen production by gassification of  
515 biomass. 2006 (PhD Dissertation) The University of Florida, USA.
- 516 [2] Escapa A, San-Martín MI, Morán A. Potential Use of Microbial Electrolysis Cells in Domestic  
517 Wastewater Treatment Plants for Energy Recovery. *Front Energy Res* 2014;2:1–10.  
518 doi:10.3389/fenrg.2014.00019.
- 519 [3] Liu H, Grot S, Logan BE. Electrochemically assisted microbial production of hydrogen from  
520 acetate. *Environ Sci Technol* 2005;39:4317–20. doi:10.1021/es050244p.
- 521 [4] Logan BE, Call D, Cheng S, Hamelers HVM, Sleutels THJA, Jeremiassse AW, et al. Microbial  
522 Electrolysis Cells for High Yield Hydrogen Gas Production from Organic Matter. *Environ Sci*  
523 *Technol* 2008;42:8630–40. doi:10.1021/es801553z.
- 524 [5] Khan MZ, Nizami AS, Rehan M, Ouda OKM, Sultana S, Ismail IM, et al. Microbial electrolysis  
525 cells for hydrogen production and urban wastewater treatment: A case study of Saudi Arabia. *Appl*  
526 *Energy* 2017;185:410–20. doi:10.1016/j.apenergy.2016.11.005.
- 527 [6] Rozendal RA, Hamelers HVM, Euverink GJW, Metz SJ, Buisman CJN. Principle and perspectives  
528 of hydrogen production through biocatalyzed electrolysis. *Int J Hydrogen Energy* 2006;31:1632–  
529 40. doi:10.1016/j.ijhydene.2005.12.006.
- 530 [7] Ivanov I, Ahn Y, Poirson T, Hickner MA, Logan BE. Comparison of cathode catalyst binders for  
531 the hydrogen evolution reaction in microbial electrolysis cells. *Int J Hydrogen Energy*  
532 2017;42:15739–44. doi:10.1016/j.ijhydene.2017.05.089.
- 533 [8] Jiang Y, Liang P, Zhang C, Bian Y, Sun X, Zhang H, et al. Periodic polarity reversal for stabilizing  
534 the pH in two-chamber microbial electrolysis cells. *Appl Energy* 2016;165:670–5.  
535 doi:10.1016/j.apenergy.2016.01.001.
- 536 [9] Zhen G, Lu X, Kumar G, Bakonyi P, Xu K, Zhao Y. Microbial electrolysis cell platform for  
537 simultaneous waste biorefinery and clean electrofuels generation: Current situation, challenges and  
538 future perspectives. *Prog Energy Combust Sci* 2017;63:119–45. doi:10.1016/j.peccs.2017.07.003.
- 539 [10] Hassan M, Xie B. Use of aged refuse-based bioreactor/biofilter for landfill leachate treatment. *Appl*  
540 *Microbiol Biotechnol* 2014. doi:10.1007/s00253-014-5813-5.
- 541 [11] Hassan M, Zhao Y XB. Employing TiO<sub>2</sub> photocatalysis to deal with landfill leachate: Current  
542 status and development. *Chem Eng J* 2016;285:264–75.
- 543 [12] Mahmoud M, Parameswaran P, Torres CI, Rittmann BE. Fermentation pre-treatment of landfill  
544 leachate for enhanced electron recovery in a microbial electrolysis cell. *Bioresour Technol*  
545 2014;151:151–8. doi:10.1016/j.biortech.2013.10.053.
- 546 [13] Mahmoud M, Parameswaran P, Torres CI, Rittmann BE. Relieving the fermentation inhibition  
547 enables high electron recovery from landfill leachate in a microbial electrolysis cell. *RSC Adv*  
548 2016;6:6658–64. doi:10.1039/C5RA25918E.
- 549 [14] Kargi F, Catalkaya EC. Electrohydrolysis of landfill leachate organics for hydrogen gas production  
550 and COD removal. *Int J Hydrogen Energy* 2011;36:8252–60. doi:10.1016/j.ijhydene.2011.04.197.
- 551 [15] Escapa A, Lobato A, García DM, Morán A. Hydrogen production and COD elimination rate in a  
552 continuous microbial electrolysis cell: The influence of hydraulic retention time and applied  
553 voltage. *Environ Prog Sustain Energy* 2013;32:263–8. doi:10.1002/ep.11619.
- 554 [16] Moreno R, San-Martín MI, Escapa A, Morán A. Domestic wastewater treatment in parallel with  
555 methane production in a microbial electrolysis cell. *Renew Energy* 2016;93:442–8.  
556 doi:10.1016/j.renene.2016.02.083.
- 557 [17] Rowe RK, Hsuan YG, Islam MZ. Leachate chemical composition effects on OIT depletion in an  
558 HDPE geomembrane. *Geosynth Int* 2008;15:136–51. doi:10.1680/gein.2008.15.2.136.
- 559 [18] Martínez EJ, Fierro J, Sánchez ME, Gómez X. Anaerobic co-digestion of FOG and sewage sludge:  
560 Study of the process by Fourier transform infrared spectroscopy. *Int Biodeterior Biodegradation*  
561 2012;75:1–6. doi:10.1016/j.ibiod.2012.07.015.
- 562 [19] Escapa A, San-Martin MI, Mateos R, Moran A. Scaling-up of membraneless microbial electrolysis  
563 cells (MECs) for domestic wastewater treatment: Bottlenecks and limitations. *Bioresour Technol*  
564 2015;180:72–8. doi:10.1016/j.biortech.2014.12.096.



- 565 [20] Heidrich ES, Dolfing J, Scott K, Edwards SR, Jones C, Curtis TP. Production of hydrogen from  
566 domestic wastewater in a pilot-scale microbial electrolysis cell. *Appl Microbiol Biotechnol*  
567 2013;97:6979–89. doi:10.1007/s00253-012-4456-7.
- 568 [21] Haddadi S, Nabi-Bidhendi G, Mehrdadi N. Nitrogen removal from wastewater through microbial  
569 electrolysis cells and cation exchange membrane. *J Environ Heal Sci Eng* 2014;12:48.  
570 doi:10.1186/2052-336X-12-48.
- 571 [22] Ivanov I, Ren L, Siegert M, Logan BE. A quantitative method to evaluate microbial electrolysis  
572 cell effectiveness for energy recovery and wastewater treatment. *Int J Hydrogen Energy*  
573 2013;38:13135–42. doi:10.1016/j.ijhydene.2013.07.123.
- 574 [23] Gil-Carrera L, Escapa A, Carracedo B, Moran A, Gomez X. Performance of a semi-pilot tubular  
575 microbial electrolysis cell (MEC) under several hydraulic retention times and applied voltages.  
576 *Bioresour Technol* 2013;146:63–9. doi:10.1016/j.biortech.2013.07.020.
- 577 [24] Hassan M, Wei H, Qiu H, Wajahat S, Jaafry H, Su Y, et al. Bioresource Technology Power  
578 generation and pollutants removal from landfill leachate in microbial fuel cell : Variation and in fl  
579 uence of anodic microbiomes 2017. doi:10.1016/j.biortech.2017.09.124.
- 580 [25] Rozendal RA, Hamelers HVM, Rabaey K, Keller J, Buisman CJN. Towards practical  
581 implementation of bioelectrochemical wastewater treatment. *Trends Biotechnol* 2008;26:450–9.  
582 doi:10.1016/j.tibtech.2008.04.008.
- 583 [26] Villano M, Scardala S, Aulenta F, Majone M. Carbon and nitrogen removal and enhanced methane  
584 production in a microbial electrolysis cell. *Bioresour Technol* 2013;130:366–71.  
585 doi:10.1016/j.biortech.2012.11.080.
- 586 [27] Zhan G, Zhang L, Li D, Su W, Tao Y, Qian J. Autotrophic nitrogen removal from ammonium at  
587 low applied voltage in a single-compartment microbial electrolysis cell. *Bioresour Technol*  
588 2012;116:271–7. doi:10.1016/j.biortech.2012.02.131.
- 589 [28] Hussain A, Manuel M, Tartakovsky B. A comparison of simultaneous organic carbon and nitrogen  
590 removal in microbial fuel cells and microbial electrolysis cells. *J Environ Manage* 2016;173:23–33.  
591 doi:10.1016/j.jenvman.2016.02.025.
- 592 [29] Kyazze G, Popov A, Dinsdale R, Esteves S, Hawkes F, Premier G, et al. Influence of catholyte pH  
593 and temperature on hydrogen production from acetate using a two chamber concentric tubular  
594 microbial electrolysis cell. *Int J Hydrogen Energy* 2010;35:7716–22.  
595 doi:10.1016/j.ijhydene.2010.05.036.
- 596 [30] Omidi H, Sathasivan A. Optimal temperature for microbes in an acetate fed microbial electrolysis  
597 cell (MEC). *Int Biodeterior Biodegrad* 2013;85:688–92. doi:10.1016/j.ibiod.2013.05.026.
- 598 [31] Clauwaert P, Tolêdo R, van der Ha D, Crab R, Verstraete W, Hu H, et al. Combining biocatalyzed  
599 electrolysis with anaerobic digestion. *Water Sci Technol* 2008;57:575–9.  
600 doi:10.2166/wst.2008.084.
- 601 [32] Hatzell MC, Kim Y, Logan BE. Powering microbial electrolysis cells by capacitor circuits charged  
602 using microbial fuel cell. *J Power Sources* 2013;229:198–202. doi:10.1016/j.jpowsour.2012.12.006.
- 603 [33] Wagner RC, Regan JM, Oh SE, Zuo Y, Logan BE. Hydrogen and methane production from swine  
604 wastewater using microbial electrolysis cells. *Water Res* 2009;43:1480–8.  
605 doi:10.1016/j.watres.2008.12.037.
- 606 [34] Tice RC, Kim Y. Methanogenesis control by electrolytic oxygen production in microbial  
607 electrolysis cells. *Int J Hydrogen Energy* 2014;39:3079–86. doi:10.1016/j.ijhydene.2013.12.103.
- 608 [35] Guo K, Tang X, Du Z, Li H. Hydrogen production from acetate in a cathode-on-top single-chamber  
609 microbial electrolysis cell with a mipor cathode. *Biochem Eng J* 2010;51:48–52.  
610 doi:10.1016/j.bej.2010.05.001.
- 611 [36] Linji X, Wenzong L, Yining W, Aijie W, Shuai L, Wei J. Optimizing external voltage for enhanced  
612 energy recovery from sludge fermentation liquid in microbial electrolysis cell. *Int. J. Hydrogen*  
613 *Energy*, vol. 38, 2013, p. 15801–6. doi:10.1016/j.ijhydene.2013.05.084.
- 614 [37] Pant D, Singh A, Van Bogaert G, Gallego YA, Diels L, Vanbroekhoven K. An introduction to the  
615 life cycle assessment (LCA) of bioelectrochemical systems (BES) for sustainable energy and  
616 product generation: Relevance and key aspects. *Renew Sustain Energy Rev* 2011;15:1305–13.  
617 doi:10.1016/j.rser.2010.10.005.
- 618 [38] Selemba PA. Microbial Electrolysis Cells: Hydrogen production from glycerol and alternative

- 619 cathode materials. 2010.
- 620 [39] Batlle-Vilanova P, Puig S, Gonzalez-Olmos R, Vilajeliu-Pons A, Bañeras L, Balaguer MD, et al.
- 621 Assessment of biotic and abiotic graphite cathodes for hydrogen production in microbial
- 622 electrolysis cells. *Int J Hydrogen Energy* 2014;39:1297–305. doi:10.1016/j.ijhydene.2013.11.017.
- 623 [40] Cusick RD, Kiely PD, Logan BE. A monetary comparison of energy recovered from microbial fuel
- 624 cells and microbial electrolysis cells fed winery or domestic wastewaters. *Int J Hydrogen Energy*
- 625 2010;35:8855–61. doi:10.1016/j.ijhydene.2010.06.077.
- 626 [41] Yong YC, Dong XC, Chan-Park MB, Song H, Chen P. Macroporous and monolithic anode based
- 627 on polyaniline hybridized three-dimensional Graphene for high-performance microbial fuel cells.
- 628 *ACS Nano* 2012;6:2394–400. doi:10.1021/nn204656d.
- 629 [42] Montpart N, Rago L, Baeza JA, Guisasaola A. Hydrogen production in single chamber microbial
- 630 electrolysis cells with different complex substrates. *Water Res* 2015;68:601–15.
- 631 doi:10.1016/j.watres.2014.10.026.
- 632 [43] Zhen G, Kobayashi T, Lu X, Kumar G, Hu Y, Bakonyi P, et al. Recovery of biohydrogen in a
- 633 single-chamber microbial electrohydrogenesis cell using liquid fraction of pressed municipal solid
- 634 waste (LPW) as substrate. *Int J Hydrogen Energy* 2016;41:17896–906.
- 635 doi:10.1016/j.ijhydene.2016.07.112.
- 636 [44] Tenca A, Cusick RD, Schievano A, Oberti R, Logan BE. Evaluation of low cost cathode materials
- 637 for treatment of industrial and food processing wastewater using microbial electrolysis cells. *Int J*
- 638 *Hydrogen Energy* 2013;38:1859–65. doi:10.1016/j.ijhydene.2012.11.103.
- 639 [45] Lu L, Xing D, Liu B, Ren N. Enhanced hydrogen production from waste activated sludge by
- 640 cascade utilization of organic matter in microbial electrolysis cells. *Water Res* 2012;46:1015–26.
- 641 doi:10.1016/j.watres.2011.11.073.
- 642 [46] Mahmoud M, Parameswaran P, Torres CI, Rittmann BE. Fermentation pre-treatment of landfill
- 643 leachate for enhanced electron recovery in a microbial electrolysis cell. *Bioresour Technol*
- 644 2014;151:151–8. doi:10.1016/j.biortech.2013.10.053.
- 645 [47] Gil-Carrera L, Escapa A, Mehta P, Santoyo G, Guiot SR, Mor??n A, et al. Microbial electrolysis
- 646 cell scale-up for combined wastewater treatment and hydrogen production. *Bioresour Technol*
- 647 2013;130:584–91. doi:10.1016/j.biortech.2012.12.062.
- 648 [48] Brettar I, Christen R, Hofle MG. *Belliella baltica* gen. nov., sp nov., a novel marine bacterium of
- 649 the Cytophaga-Flavobacterium-Bacteroides group isolated from surface water of the central Baltic
- 650 Sea. *Int J Syst Evol Microbiol* 2004;54:65–70. doi:10.1099/ijs.0.02752-0.
- 651

652 **FIGURE CAPTIONS**

653

654 **Fig 1:** Schematics of the experimental set-up.

655 **Fig 2:** Current density profiles of MEC-1 (A) and MEC-2 (B) operating at various  
656 applied potentials (batch mode). MEC-1 was operated at controlled

657 **Fig. 3:** COD removal of MEC-1 (A) and MEC-2 (B) and Nitrogen removal efficiency of  
658 MEC-1 (C) and MEC-2 (D) along various cycles in batch mode operation.

659 **Fig 4:** Energy balance and efficiency of MEC-1 (A) and MEC-2 (B).

660 **Fig. 5:** Correspondence analysis (CA) of eubacterial communities from Inoculum,  
661 MEC-1\_PI, MEC-1\_PII and MEC-1\_PIII samples, based on pyrosequencing of  
662 eubacteria *16S rRNA gene* with genus level taxonomy matrix (B): Taxonomic  
663 classification of pyrosequencing of *16S rRNA gene* from eubacterial communities at  
664 family level  
665

666 **TABLE CAPTIONS**

667 **Table 1:** Employing complex substrates in MEC.

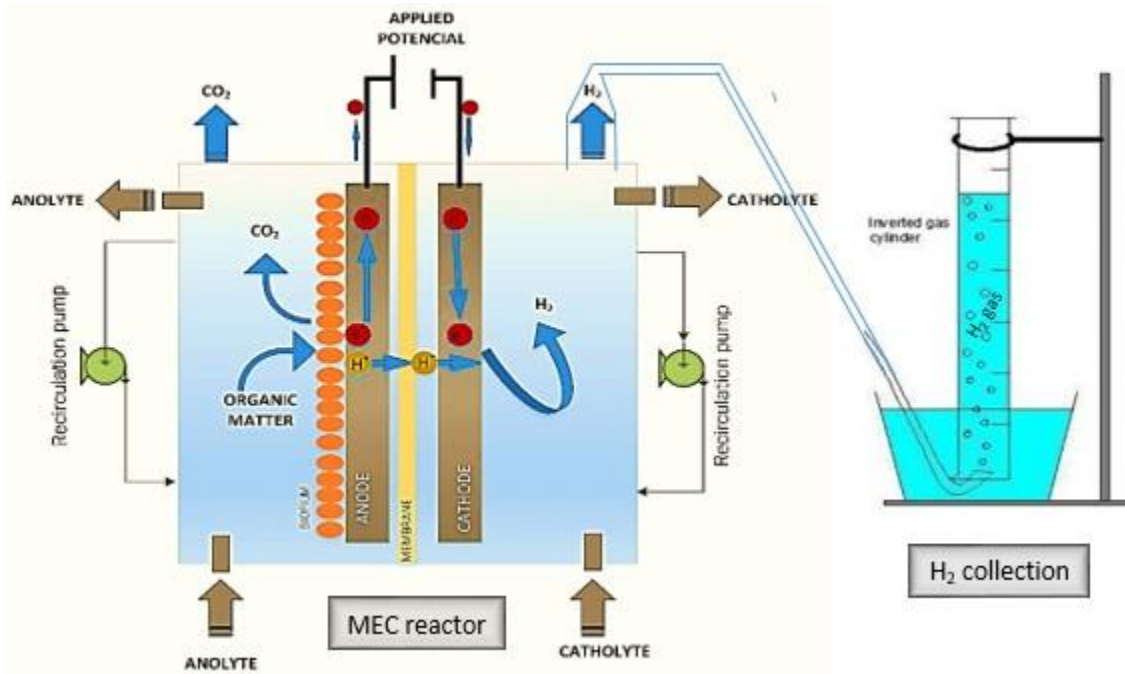
668 **Table 2:** Applied conditions for MEC-1 and MEC-2

669 **Table 3:** Chemical characteristics of simulated leachate employed in this study ( $n = 10$ )

670 **Table 4:** MEC system performance along different cycles and applied voltages ( $E_{ap}$ ) at  
671 batch mode operation

672 **Table 5:** Comparative evaluation of the results obtained in this study with other existing  
673 hydrogen producing technologies.

674 **Figures**  
675



676  
677  
678  
679 **Fig. 1:** Schematics of the experimental set-up

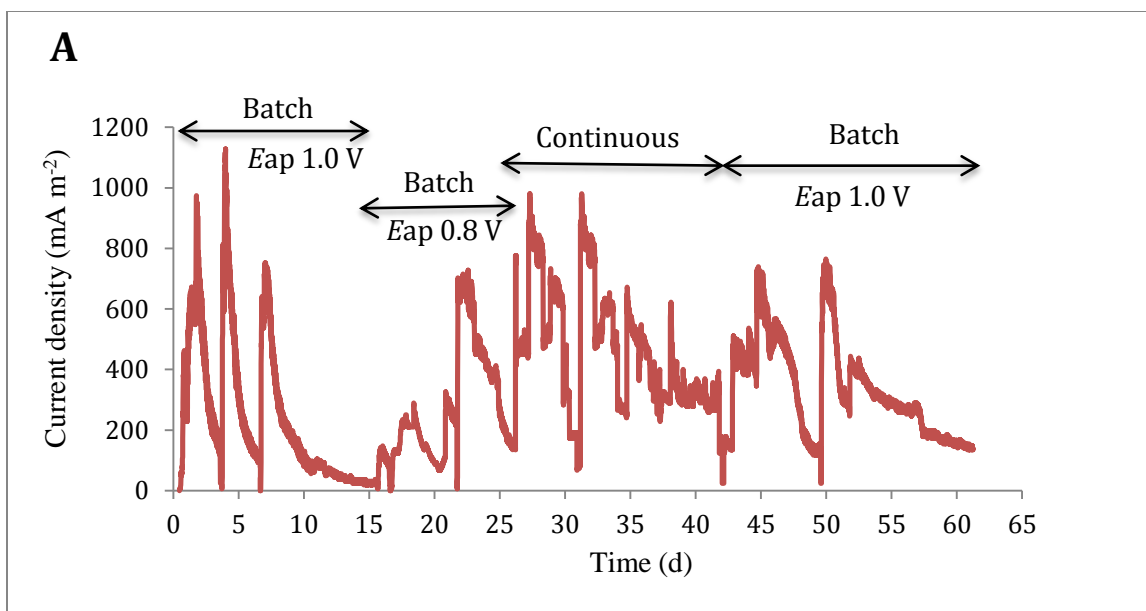
680

681

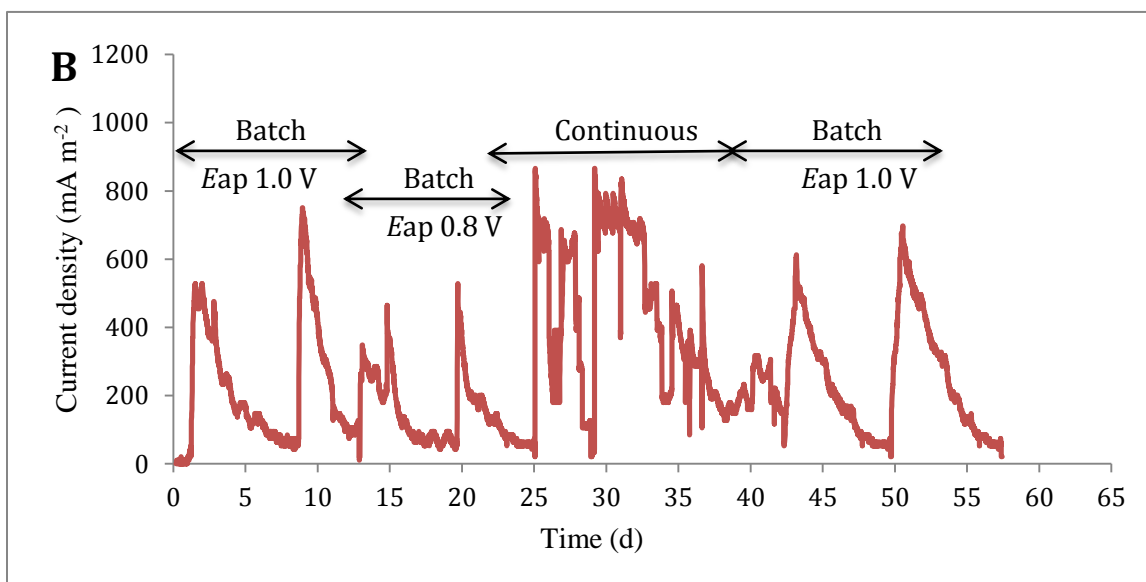
682

683

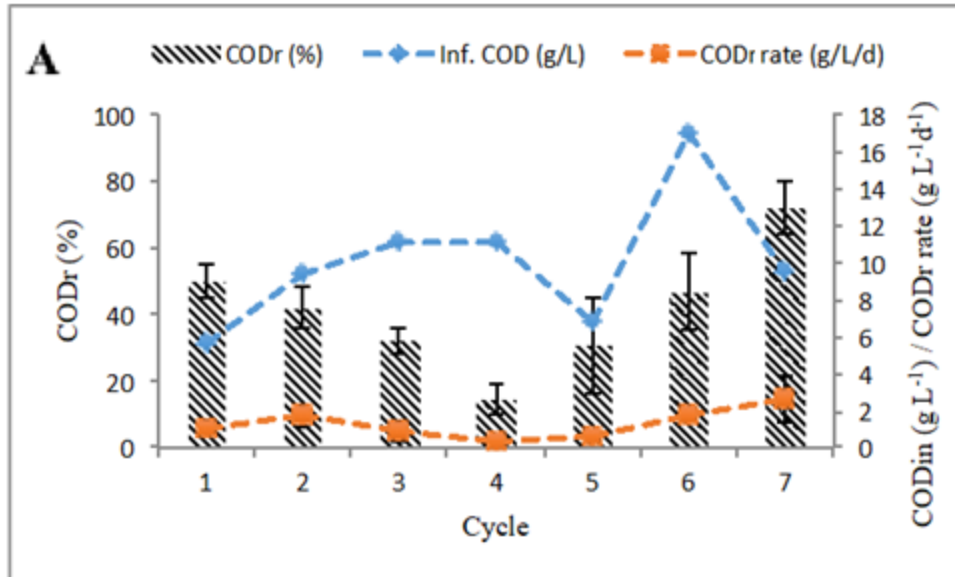
684



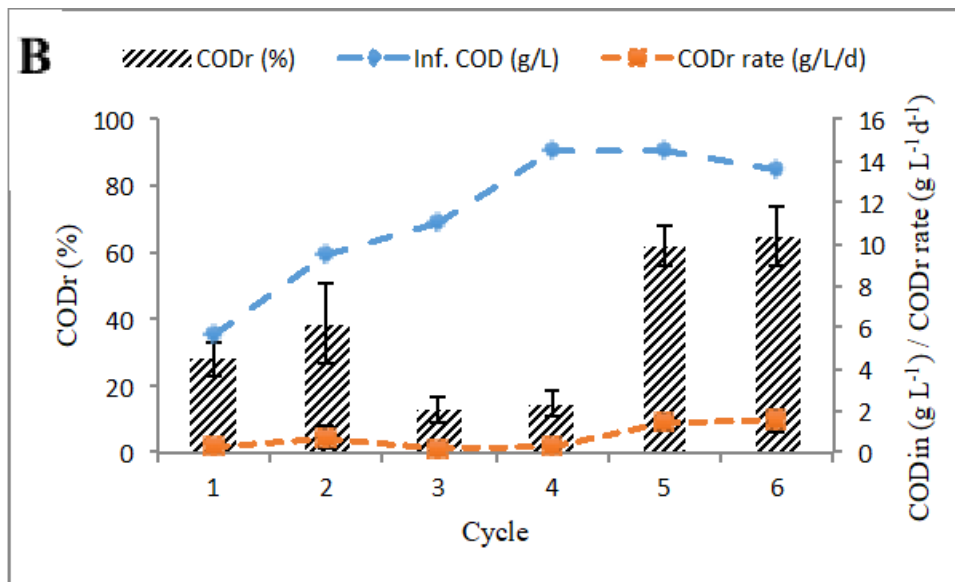
685



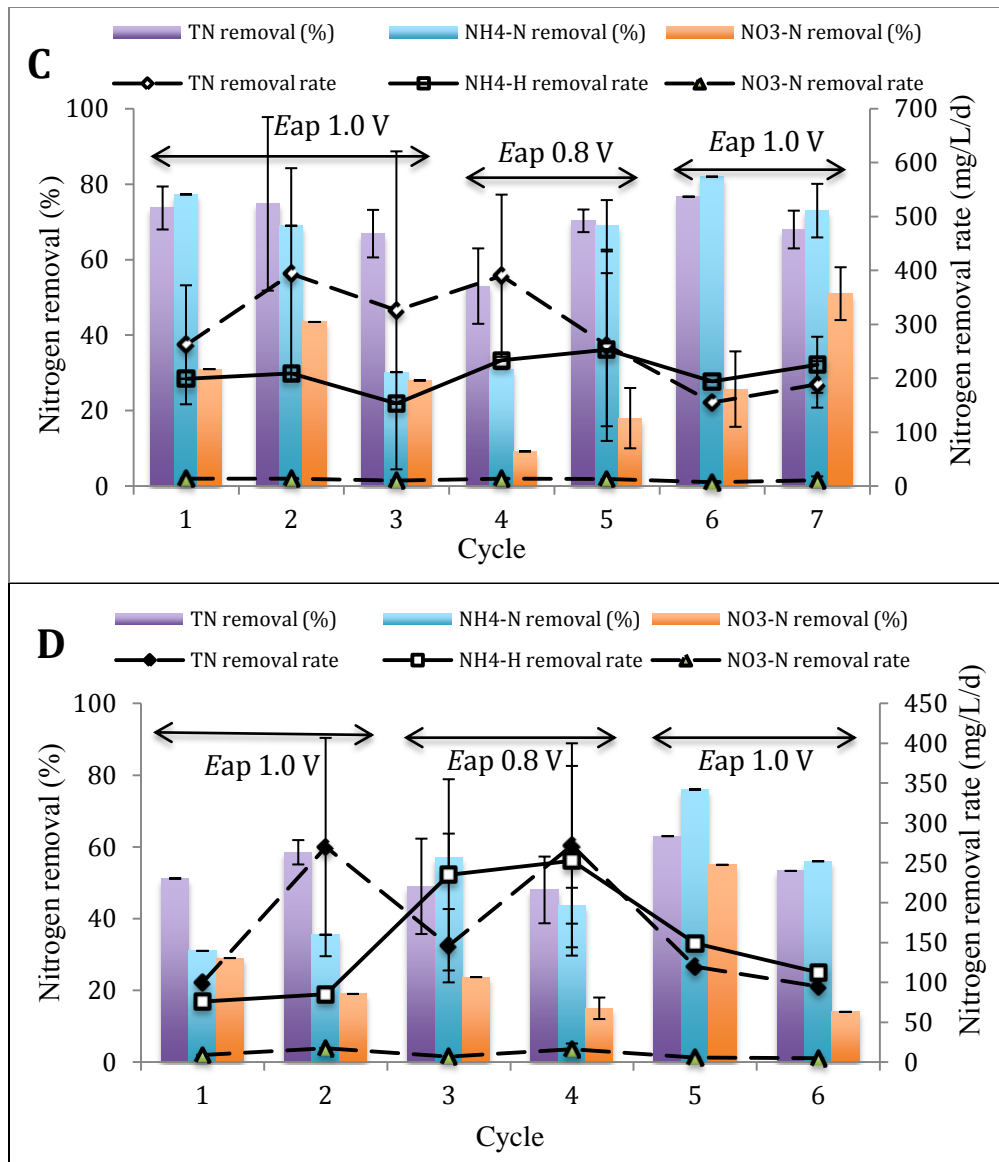
686 **Fig 2:** Current density profiles of MEC-1 (A) and MEC-2 (B) operating at various  
 687 applied potentials (batch mode). MEC-1 was operated at controlled temperature (30 °C)  
 688 and MEC-2 at room temperature ( $17 \pm 3$  °C).



689  
690



691

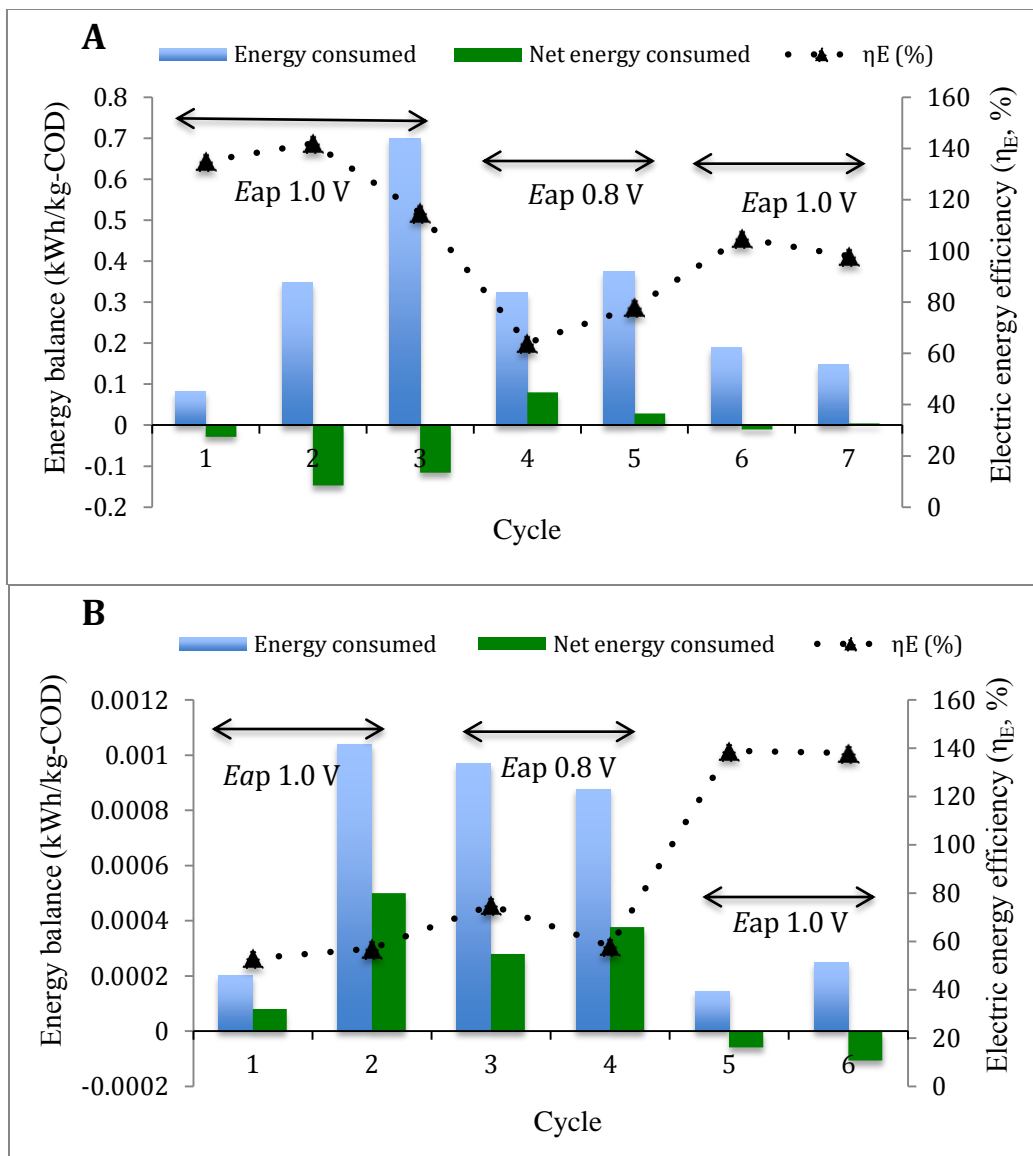


692

693  
694  
695  
696  
697  
698

**Fig 3.** COD removal of MEC-1 (A) and MEC-2 (B) and Nitrogen removal efficiency of MEC-1 (C) and MEC-2 (D) along various cycles in batch mode operation. *Eap* of all cycles are 1 V, except cycle 4 and 5, 0.8 V (A) and cycle 3 and 4 (B).

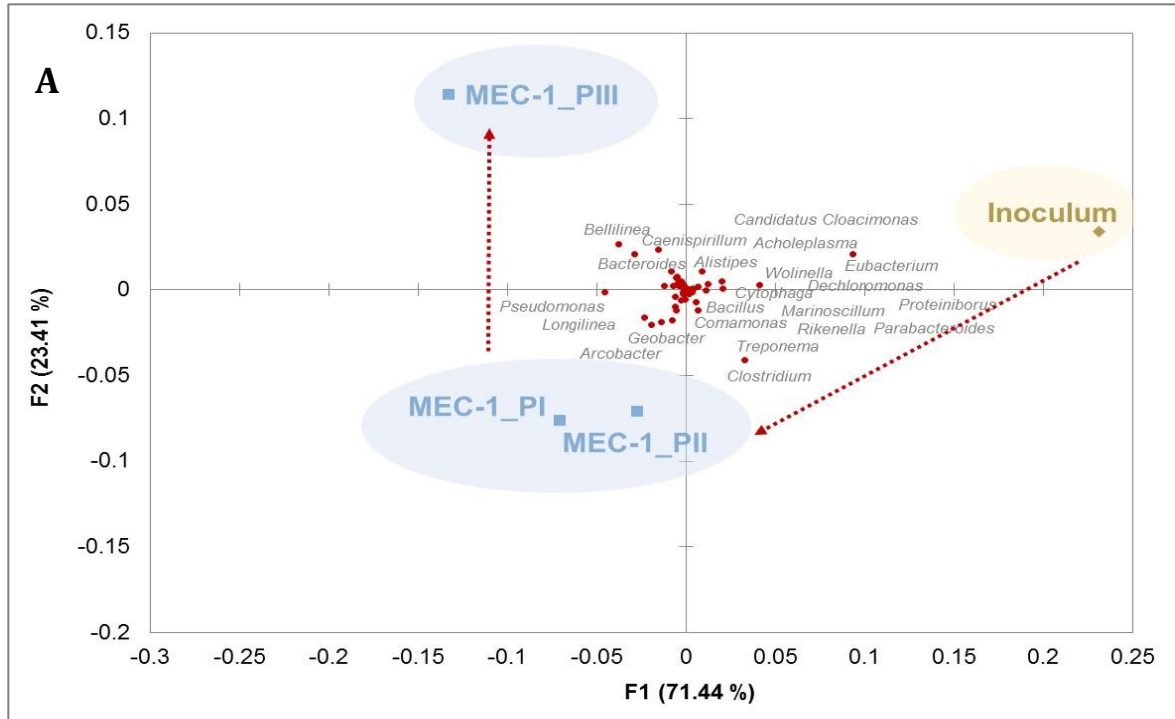
699



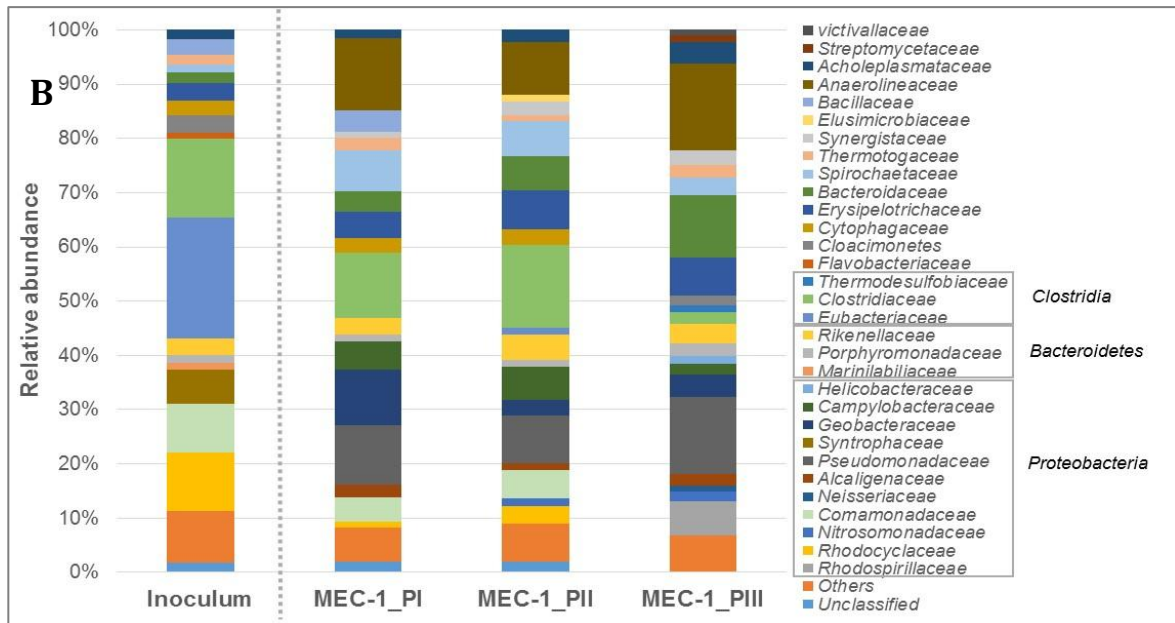
700  
701  
702  
703

**Fig. 4:** Energy balance and efficiency of MEC-1 (A) and MEC-2 (B).  $E_{ap}$  of all cycles are 1 V, except 0.8 V in cycle 3 and 4 (MEC-1) and cycle 4 and 5 (MEC-2).





704



705

706 **Fig 5. (A):** Correspondence analysis (CA) of eubacterial communities from Inoculum, MEC-  
 707 1\_PI, MEC-1\_PII and MEC-1\_PIII samples, based on pyrosequencing of eubacteria *16S rRNA*  
 708 *gene* with genus level taxonomy matrix **(B):** Taxonomic classification of pyrosequencing  
 709 of *16S rRNA gene* from eubacterial communities at family level. Sequences accounting  
 710 for less than 1% of the total reads have been included in the “Others” category.

711

712 **Tables**

713

714 **Table 1:** Employing complex substrates in MEC.

Substrate	Reactor type	Volume (mL)	$E_{ap}$ (V)	$j$ (A/m <sup>3</sup> )	CE (%)	$r_{cat}$ (%)	Biogas composition (% H <sub>2</sub> )	QH <sub>2</sub> (m <sup>3</sup> m <sup>-3</sup> .d)	Reference
Glycerol	SC	28	0.8	100	35->100	4	5	0.021	[42]
Starch	SC	28	0.8	25	35->100	0	0	0	[42]
Milk	SC	28	0.8	75	30->100	13	76	0.086	[42]
Diluted LPW	SC	100	3.0	115.9±7.2 <sup>*</sup>	118-152	5 - 21	16-50	0.12 - 0.38	[43]
Food processing	SC	280	0.7	1.0-2.4 <sup>b</sup>	29±2		32±4	0.12±0.02	[44]
Food processing	SC	280	0.7	1.2-2.1 <sup>b</sup>	12±2		86	0.8-1.8	[44]
Raw activated sludge	DC	250	-	8	28±10	69±9	n.a.	0.056±0.008	[45]
Swine WW	DC	28	0.5	106-112	29-70	29-61	58-64	0.9-1.0	[33]
Domestic WW	SC	120000	1.1	0.135 <sup>*</sup>		60	100±6.4	0.015	[20]
Landfill leachate	SC	320	-3.0 <sup>a</sup>	0.11±0.06 <sup>b</sup>	1.8±0.5	n.a.	n.d.	n.d.	[13]
Fenton-treated leachate	SC	320	-3.0 <sup>a</sup>	1.42±0.27 <sup>b</sup>	29±0.5	n.a.	n.d.	n.d.	[13]
Landfill leachate	DC	320	0.3 <sup>a</sup>	2.5	56	n.a.	n.d.	n.d.	[46]
Pre-fermented leachate	DC	320	0.3 <sup>a</sup>	23	68	n.a.	n.d.	n.d.	[46]
Domestic WW	SC	2000	1.0	0.22 <sup>b</sup>	28-30	18.6	100	0.05	[47]
Simulated landfill leachate	DC	1000	1.0	1.0-1.2 <sup>b</sup>	12-41	66-95	98	0.04±0.06	This study

715 Index \* implies that the parameter has been computed from the actual existing data in respective  
716 publication. *LPW*: Liquid fraction of pressed municipal solid waste; *SC*: Single-chambered; *DC*: Dual-  
717 chambered

718 <sup>a</sup> Anodic poised potential (V) vs Ag/AgCl

719 <sup>b</sup>  $j$  (A/m<sup>2</sup>)

720 **Table 2:** Applied conditions for MEC-1 and MEC-2

Reactor	Cycle	Operation mode	Operation time (d)	$E_{ap}$ (V)	Temperature (°C)
MEC-1	1	Batch	1-4	1.0	30
	2	Batch	5-8	1.0	30
	3	Batch	9-15	1.0	30
	4	Batch	16-20	0.8	30
	5	Batch	21-26	0.8	30
		Continuous	26-42	**	30
	6	Batch	42-50	1.0	30
	7	Batch	50-62	1.0	30
MEC-2	1	Batch	1-8	1.0	17±3
	2	Batch	9-13	1.0	17±3
	3	Batch	14-19	0.8	17±3
	4	Batch	20-25	0.8	17±3
		Continuous	26-42	**	30
	5	Batch	42-50	1.0	17±3
	6	Batch	50-68	1.0	17±3

721 \*\*  $E_{ap}$  ranging from 0.5-1.0 V

722

723 **Table 3:** Chemical characteristics of simulated landfill leachate employed in this study (*n*  
 724 = 10)  
 725

Parameter	Unit	Value ( $\pm$ Standard deviation)
pH		7.86 $\pm$ 0.63
Electrical conductivity (EC)	mS cm <sup>-1</sup>	16.11 $\pm$ 3.01
Oxidation-Reduction Potential (ORP)	mV	200.63 $\pm$ 31.72
Chemical Oxygen Demand (COD)	g L <sup>-1</sup>	14.33 $\pm$ 4.42
Total Organic Carbon (TOC)	g L <sup>-1</sup>	4.81 $\pm$ 1.31
Inorganic Carbon (IC)	g L <sup>-1</sup>	0.44 $\pm$ 0.17
Total Carbon (TC)	g L <sup>-1</sup>	5.59 $\pm$ 1.61
Total Nitrogen (TN)	g L <sup>-1</sup>	0.80 $\pm$ 0.13
Ammonium Nitrogen (NH <sub>4</sub> - N)	g L <sup>-1</sup>	0.72 $\pm$ 0.10
Nitrate Nitrogen (NO <sub>3</sub> - N)	g L <sup>-1</sup>	0.04 $\pm$ 0.01
Phosphate (PO <sub>4</sub> -P)	g L <sup>-1</sup>	0.012 $\pm$ 0.008
<i>Volatile Fatty Acids (VFAs):</i>		
– Acetic acid	g L <sup>-1</sup>	4.86 $\pm$ 1.39
– Propionic acid	g L <sup>-1</sup>	3.64 $\pm$ 0.76
– Butyric acid	g L <sup>-1</sup>	0.98 $\pm$ 0.06

726

727 **Table 4:** MEC system performance along different cycles and applied voltages ( $E_{ap}$ ) at  
 728 batch mode operation  
 729

Reactor	Cycle #	1	2	3	4	5	6	7
MEC-1	$E_{ap}$ (V)	1.0	1.0	1.0	0.8	0.8	1.0	1.0
	Cycle time (h)	85	75	230	72	189	153	115
	CE (%)	14.5	13.4	41	20	18	12	14
	$r_{cat}$ (%)	91	96	76	44	51	89	66
	$Q_{H_2}$ (L La <sup>-1</sup> d <sup>-1</sup> )	0.148±0.116	0.132±0.103	0.109±0.102	0.024±0.01	0.043±0.01	0.08±0.04	0.10±0.05
MEC-2	$E_{ap}$ (V)	1.0	1.0	0.8	0.8	1.0	1.0	
	Cycle time (h)	192	124	163	110	156	128	
	CE (%)	31	31	35.6	32.7	11	12.5	
	$r_{cat}$ (%)	21	25	39	23	120	114	
	$Q_{H_2}$ (L La <sup>-1</sup> d <sup>-1</sup> )	0.004±0.002	0.012	0.01±0.01	0.01±0.01	0.03±0.03	0.04±0.06	

730

731 **Table 5:** Comparative evaluation of the results obtained in this study with other existing  
 732 hydrogen producing technologies.

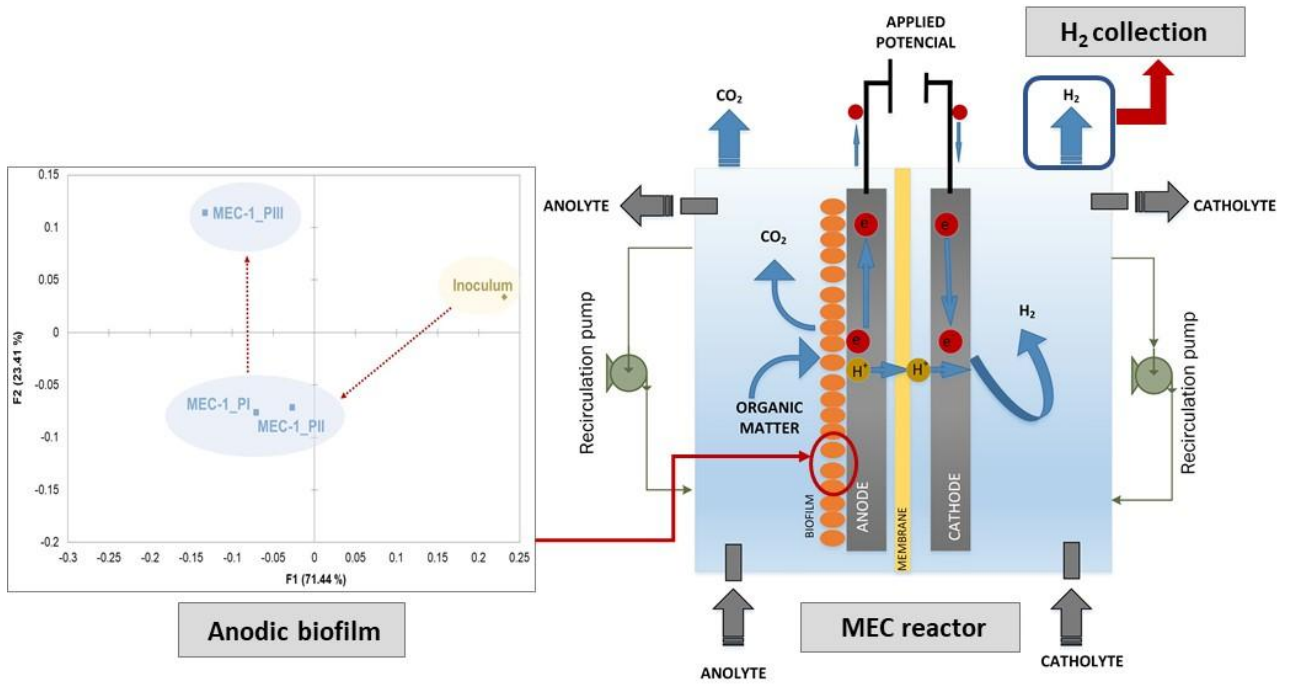
Specifics	This study	Biotic MEC	Steam methane reforming	Partial oxidation of heavy oil	Coal gasification	Grid electrolysis of water
Energy efficiency ( $\eta_E$ , %)	46 – 142	53 – 175	70 – 80	70 – 74	60	27
Energy consumption ( $\text{kWh kg}^{-1} \text{H}_2$ )	2.7 – 10.1	33.2 – 117	22.4	54.9	96.3	54.9
$\text{H}_2$ production cost ( $\text{€ kg}^{-1} \text{H}_2$ )	$0.67 \pm 0.24$	3.04	0.71	1.32	1.15 – 2.30	2.43 -2.82

733 Data obtained from Ref. [1,39,48]

734

735 **Graphical Abstract**

736



737

**Supplementary Material**

[Click here to download Supplementary Material: Supplementary Material.docx](#)